

1 **Projected water table depth changes of the world's** 2 **major groundwater basins and potential human impact**

3 **Maya Costantini¹, Jeanne Colin¹, Bertrand Decharme¹**

4 ¹Centre National de Recherches Météorologiques (CNRM), Météo-France/CNRS, Toulouse, France

5 **Key Points:**

- 6 • The impact of climate change on water table depth in the world's major groundwater
7 basins is assessed using CMIP6 global simulations.
- 8 • Projections run with four SSP scenarios show a global rising of groundwater by 2100,
9 with the occurrence of a depletion in numerous regions.
- 10 • In 2100, 31% to 40% of the world's population could face water scarcity issues or
11 flood risks worsened by these water table depth changes.

Corresponding author: Maya Costantini, maya.costantini@meteo.fr

Abstract

As groundwater found in aquifers is the main reservoir of freshwater for human activity, knowledge of the future response of groundwater to climate change is key for improving water management adaptation plans. We analyse the evolution of future levels of unconfined aquifers in the 218 world's major groundwater basins in global climate simulations following the latest IPCC scenarios, run with models able to capture feedbacks among climate, land use and groundwater. Neglecting these feedbacks has been identified by the IPCC Sixth Assessment Report (AR6) as a source of uncertainties in impact models. We find a rising of groundwater levels on global average, which is consistent with the projected global intensification of precipitation. However, the evolution of water table depths is not spatially uniform and presents large regional disparities. Depending on the scenario, we find a rise (respectively a depletion) of groundwater levels in 2100 over 40% to 52% (respectively 20% to 26%) of the area covered by the 218 world's major groundwater basins. Using spatialized projections of population in 2100, we estimate that 31% to 43% of the world's population could be affected by these groundwater changes, facing either water scarcity issues, or increased risks of flooding. As the climate models we used do not represent human groundwater withdrawals, we also use the projections of population to identify regions where groundwater withdrawals could exacerbate the projected depletion, or even reverse a projected rise into a depletion.

1 Introduction

Groundwater, stored in permeable geological structures (aquifers), constitutes the largest unfrozen reserve of freshwater on Earth. It amounts to approximately 35% of human fresh water withdrawals (Döll et al., 2012) and sustains ecosystems by supplying baseflow during dry periods. The recharge of aquifers stems mainly from rainfall, melted snow, and water exchanges with inland water bodies. Conversely, groundwater sustains these bodies of water and is the main driver of river flow. To a lesser extent, it also contributes to evapotranspiration in groundwater-dependent ecosystems. In addition to these natural water fluxes, pumping and soil infiltration of irrigation water also affect groundwater levels. The evolution of groundwater resources with climate change is therefore of great importance for both humankind and natural ecosystems.

As climate change modify the natural hydrological cycle as well as human water use and demand, it also affect groundwater resources (Green et al., 2011; R. G. Taylor et al., 2013; Wada, 2016; Scanlon et al., 2012; IPCC, 2021c). Over the past decade, studies exploring the impact of future climate change on groundwater have relied on hydrological models driven by atmospheric forcing or estimated recharge. Until the recent work of Wu et al. (2020), who used a fully coupled global climate model, studies exploring the impacts of future climate change on groundwater have relied on hydrological models driven by atmospheric forcings or estimated recharges. Few of these studies are global (Wada et al., 2012; Reinecke et al., 2021). In most cases, the spatial scale is limited to a given set of watershed or a single region (Meixner et al., 2016; Maxwell & Kollet, 2008; Condon et al., 2020; Amanambu et al., 2020). These global and regional studies give valuable insights regarding the future of groundwater resources, but regardless of their scale, they can not take account the groundwater-climate feedbacks because of their modelling framework. Without these feedbacks, the response of groundwater to climate change may be biased (Maxwell & Kollet, 2008; Meixner et al., 2016), and the future long-term evolution of the land surface hydrology can be misleading (Boé, 2021).

Over the past few years, a number of authors have recommended the inclusion of a representation of groundwater in Earth system models and global climate models (Clark et al., 2015; Fan et al., 2019; Boé, 2021; Gleeson et al., 2021), and some of them have argued that these integrated models would ultimately help to assess the future effects of

62 climate change on groundwater (Fan et al., 2019; Gleeson et al., 2021). Taking up this
63 suggestion, Wu et al. (2020) considered an ensemble of future global simulations following
64 the old business-as-usual RCP8.5 scenario (designed for the fifth phase of the Coupled
65 Model Intercomparison Project CMIP5 (K. E. Taylor et al., 2012)), performed with the
66 Community Earth System Model version 4.0 (Kay et al., 2015) which includes a simple
67 parameterization of aquifers. The authors analysed the future evolution of groundwater
68 storage in this ensemble of projections, but they limited their assessment to 7 key mid-
69 latitudes aquifers, thus failing to provide a worldwide picture of the global changes.

70 In this present study, we look to go beyond the work of Wu et al. (2020) by providing
71 a wider scale analysis of future groundwater levels using more recent global climate simu-
72 lations. To do so, we consider the future evolution of the 218 world's major groundwater
73 basins which cover 43% of the global land surface (without Antarctica and Greenland) and
74 under four of the up-to-date greenhouse gas concentration pathways scenarios (SSP126,
75 SSP245, SSP370 and SSP585) (O'Neill et al., 2017). The simulations were performed at
76 the French National Center for Meteorological Research (CNRM in french), for the sixth
77 phase of the Coupled Model Intercomparison Project (CMIP6) (Eyring et al., 2016) with our
78 two fully coupled climate models CNRM-CM6-1 (Voltaire et al., 2019) and CNRM-ESM2-1
79 (Séférián et al., 2019). Both models include a hydrogeological representation of unconfined
80 aquifer processes in the world's major groundwater basins (Decharme et al., 2019; Vergnes
81 & Decharme, 2012). They simulate the evolution of the Water Table Depth (WTD), de-
82 fined as the depth of the piezometric head in each aquifer, using a two-dimensional diffusive
83 scheme of the groundwater flows also accounting for two-way water exchanges with the
84 river and the unsaturated soil column. This two-way coupling allows the CNRM models to
85 capture groundwater-climate feedback, and CNRM-ESM2-1 accounts for land-use changes
86 feedbacks.

87 The recently issued IPCC Sixth Assessment Report (AR6) (IPCC, 2022a) pointed out
88 the necessity to include such feedbacks in projections of future groundwater resources. With
89 the inclusion of these processes in the CNRM models, the present study contributes to
90 further narrow one of the knowledge gaps identified in the AR6 (IPCC, 2022a). However,
91 human groundwater withdrawals and irrigation are not simulated in the CNRM models, as is
92 also the case for most of the models used in the previously mentioned studies. Therefore, our
93 analysis only considers the "natural" part of the climate change-induced changes of water
94 table depths. It constitutes a first step in the evaluation of the climate change impacts on
95 future groundwater resources.

96 Hereafter, the evolution of WTD is analysed over the 1850-2100 period using CMIP6
97 simulations run with the CNRM models. The results are put in perspective with a multi-
98 model analysis of the precipitation and evapotranspiration changes simulated by 18 other
99 state-of-the-art global climate models which contributed to CMIP6. Finally, we discuss the
100 foreseeable impacts of the projected evolution of groundwater levels on the human water
101 need in 2100, and vice versa.

102 **2 Materials and Methods**

103 **2.1 CNRM models**

104 The global climate model CNRM-CM6-1 (<http://www.umr-cnrm.fr/cmip6/spip.php?article11>) and the Earth system model CNRM-ESM2-1 (<http://www.umr-cnrm.fr/cmip6/spip.php?article10>) are both two global fully coupled atmosphere-ocean-surface
105 general circulation models of the CNRM. They are part of the models engaged in CMIP6
106 to contribute to the AR6 (Eyring et al., 2016; IPCC, 2021a). These models are run at
107
108

109 a resolution of approximately 1.5° and based on the same core of components. CNRM-
110 CM6-1 simulates the main physical processes in the ocean, the sea ice, the land surface
111 and the atmosphere (Voldoire et al., 2019). Using the same physics, CNRM-ESM2-1 repre-
112 sents in addition the global carbon cycle including carbon cycling in vegetation. Leaf level
113 photosynthesis, plant respiration, stomatal conductance, and plant biomass are explicitly
114 computed by the model. Leaf phenology results directly from the simulated carbon bal-
115 ance of the canopy (Delire et al., 2020). This allows to represent the physiological effects
116 of CO_2 on plant transpiration and growth (increased water use efficiency and fertilisation
117 effect). CNRM-ESM2-1 also accounts for land-use-land-cover change scenarios derived from
118 the Land Use Harmonized version 2 release LUH2 (Hurtt et al., 2020) for CMIP6 and in-
119 cludes an interactive atmospheric chemistry scheme and an interactive tropospheric aerosols
120 scheme (S  f  rian et al., 2019).

121 In these two climate models, the ISBA-CTRIP (Decharme et al., 2019) (Interaction-
122 Soil-Biosphere-Atmosphere - CNRM version of the Total Runoff Integrating Pathways) land
123 surface system provides a physical and realistic representation of the continental hydrolog-
124 y (<http://www.umr-cnrm.fr/spip.php?article1092&lang=en>). ISBA uses multilayer
125 schemes for both the soil and the snowpack to calculate the time evolution of the water
126 and energy budgets at the land surface and to provide water flow to CTRIP. In this way,
127 CTRIP which simulates inundation dynamic, groundwater processes and river discharges in
128 the ocean. Because of the coarse resolution of the model (0.5°), only the 218 world's largest
129 unconfined aquifer basins with diffusive groundwater movements are represented for the mo-
130 ment (Vergnes & Decharme, 2012; Vergnes et al., 2012). More complex aquifer systems like
131 confined, karstic, orogenic and localized shallow aquifers remain difficult to simulate at the
132 global scale due to the lack of precise global parameter database. The hydrogeological mod-
133 elling of groundwater dynamics relies on a two-dimensional one-layer diffusive widespread
134 unconfined aquifer scheme (Vergnes et al., 2012) based on the well-known MODCOU hy-
135 drogeological model (Vergnes, May 2014; Ledoux et al., 1989). This scheme computes the
136 WTD in aquifers according to the lateral groundwater fluxes, the two-way water exchanges
137 with the rivers (Vergnes & Decharme, 2012; Vergnes et al., 2012) and the unsaturated soil
138 (Decharme et al., 2019; Vergnes J.P., Decharme B, 2014). Groundwater basins boundaries
139 and their hydrogeological parameters were estimated using global maps of groundwater re-
140 sources and topological, lithological and geological data sets (Vergnes & Decharme, 2012).
141 Groundwater basins have been delimited using the global map of the groundwater resources
142 of the world from the Worldwide Hydrogeological Mapping and Assessment Programme
143 (WHYMAP), the hydrogeological map over the United States from the U.S. Geological Sur-
144 vey (USGS) and the global map of lithology (D  rr et al., 2005). This last map also allows
145 one to determine the transmissivity and the effective porosity in each aquifer basin (Vergnes
146 & Decharme, 2012; Decharme et al., 2019).

147 Groundwater processes as well as other hydrological features were validated thoroughly
148 during the last decade in ISBA-CTRIP on a regional and global scale. These evaluations
149 were performed specifically by comparing model results to in-situ measurements of the
150 piezometric head, the GRACE terrestrial water storage estimates and a large set of in-situ
151 river discharges measurements in forced land surface applications (Decharme et al., 2019;
152 Vergnes & Decharme, 2012; Vergnes et al., 2012; Vergnes J.P., Decharme B, 2014) as well as
153 in our fully-coupled climate models (Voldoire et al., 2019; Roehrig et al., 2020). Finally, it
154 was thanks to this evaluation work that the ISBA-CTRIP land surface system was used in
155 many global hydrological applications, some of which highlight important results regarding
156 global hydrology and climate change (Padr  n et al., 2020; Cazenave et al., 2014; Douville
157 et al., 2013).

158 In this study, we only consider the WTD which are shallower than 100 *m* ($WTD <$
159 $100m$) over 1985–2014 in the historical CMIP6 experiment (present-day climate). In deeper
160 aquifers, we assume that groundwater is too disconnected from the surface to be significantly

161 impacted by climate change at the time scales we consider (less than 250 years). This is
 162 especially true over hyper-arid regions (e.g. in the Sahara desert) where fossil aquifers were
 163 recharged by precipitation during paleoclimatic periods (R. G. Taylor et al., 2013; Scanlon
 164 et al., 2006; Alley et al., 2002). The current annual precipitation rates here are extremely
 165 weak, which limits the groundwater recharge and thus constrains WTD to very deep levels.

166 2.2 CMIP6 Experiments and Data Post-processing

167 Our analysis of the water table depth changes is based on the results of CMIP6 simula-
 168 tions which were run with the CNRM models. The multi-model analysis includes the results
 169 of CMIP6 simulations run with the 18 models of the CMIP6 panel which had published the
 170 variables of interest (see next subsection) at the time of our analysis (see Table 1). For the
 171 past and present-day climate (1850 – 2014) we use simulations run for the historical exper-
 172 iment, which is part of the CMIP6 core experiments (Eyring et al., 2016). For the future
 173 period (2015 – 2100), we use simulations run for the ScenarioMIP experiments (O’Neill et
 174 al., 2016, 2017; Meinshausen et al., 2017). We consider four scenarios, based on different
 175 Shared Socioeconomic Pathways (SSP) and different levels of radiative forcing (increase of
 176 the atmosphere’s radiative balance (in $W.m^{-2}$) between 1850 and 2100) : SSP126, SSP145,
 177 SSP370, SSP585. To put it simply, the SSP126 scenario is the optimistic one. It is defined
 178 by a sustainable societal development, with a relatively low radiative forcing. The SSP245
 179 scenario is a middle-of-the-road pathway. It depicts a world where the socioeconomic trends
 180 do not deviate too much from the historical period patterns, with an intermediate radiative
 181 forcing. The SSP370 scenario displays regional rivalries and a higher radiative forcing. The
 182 SSP585 scenario in the worst case scenario, with a strong fossil-fueled development and a
 183 subsequently high radiative forcing.

184 For each experiment (historical or scenarios), models run an ensemble of simulations,
 185 composed of several members. These ensembles allows to sample the climate internal vari-
 186 ability and thus provides a better assessment the models’ response to the evolution of climate
 187 forcings (the more members, the better). We used all the available members at the time
 188 of our analysis (see Table 1). The variables we considered are the Water Table Depth
 189 (*WTD*), precipitation (*PR*) and evapotranspiration (*EVSPSBL*). As the two CNRM
 190 climate models provide similar results for the variables of interest, their data were pro-
 191 cessed jointly. The same weight was given to CNRM-CM6-1 and CNRM-ESM2-1 by first
 192 computing the ensemble mean of each model (average of all members) for each variable
 193 and each experiment, and then averaging the two ensemble means. For the multi-model
 194 analysis of the 18 other state-of-the-art CMIP6 models we considered, we also computed
 195 the ensemble means of each model, and then we averaged these ensemble means. All the
 196 variables computed by the different CMIP6 models were regridded on the 0.5 regular grid
 197 over which *WTD* is computed in the CNRM models. The interpolation was done us-
 198 ing a first order conservative remapping provided by the Climate Data Operator (CDO:
 199 <http://www.idris.fr/media/ada/cdo.pdf>). The interpolation was performed on the en-
 200 semble means of each model, as were any further statistical computations (time series,
 201 averages over time periods, percentages of change, etc.).

Table 1. Models used and number of members for each model

Global Climate Model	Number of members (historical)	Number of members (SSPs)
<i>CNRM/CNRM – CM6 – 1</i>	30	6
<i>CNRM/CNRM – EMS2 – 1</i>	11	5
<i>BCC/BCC – CSM2 – MR</i>	3	1
<i>CAS/FGOALS – f3 – L</i>	3	3
<i>CAS/FGOALS – g3</i>	6	4
<i>CCCma/CanESM5 – CanOE</i>	3	3
<i>CCCma/CanESM5</i>	40	25
<i>CSIRO/ACCESS – ESM1 – 5</i>	10	3
<i>INM/INM – CM4 – 8</i>	1	1
<i>INM/INM – CM5 – 0</i>	10	1
<i>IPSL/IPSL – CM6A – LR</i>	32	6
<i>MIROC/MIROC6</i>	50	50
<i>MIROC/MIROC – ES2L</i>	10	1
<i>MOHC/UKESM1 – 0 – LL</i>	11	5
<i>NASA – GISS/GISS – E2 – 1 – G</i>	10	1
<i>NCAR/CESM2</i>	11	5
<i>NCAR/CESM2 – WACCM</i>	3	5
<i>NIMS – KMA/KAGE – 1 – 0 – G</i>	3	3
<i>NOAA – GFDL/GFDL – ESM4</i>	2	1
<i>UA/MCM – UA – 1 – 0</i>	1	1

202 The statistical significance of field differences on maps computed using the False Detection
 203 Rate (FDR) test (Wilks, 2006, 2016). The FDR test is based on a Student test for the
 204 computation of P-values at each grid point. To determine the significance, P-values are com-
 205 pared to a threshold which depends on the series of P-values (for every grid point). This test
 206 allows to reduce the rate of false significance, which can be rather high for auto-correlated
 207 fields such as climate variables ((Wilks, 2006, 2016)).

208 **2.3 Future Population Density Projections**

209 The evolution of population density (people per km²) is derived from the projection
 210 of population density by countries (KC & Lutz, 2017) conducted for CMIP6 and with the
 211 population density in 2015 at 0.5° provided by the SocioEconomic Data and Applications
 212 Center (SEDAC, 2018). For each country, the percentage of change in population density is
 213 computed between 2015 and 2100 according to CMIP6 projections. This percentage is then
 214 applied to the population density at 0.5° in 2015 provided by the SEDAC.
 215

216 **3 Results**

217 **3.1 Current status and projected groundwater levels**

218 The current status of the world's major groundwater basins simulated by the CNRM
 219 models is shown in Fig.1. 40% of the global land area presents a WTD which is shallower
 220 than 100 *m* and 36% of the land area presents WTD between 1 and 10 *m*. This is consistent
 221 with estimates from the high resolution observation-driven model of Fan et al. (2013) based
 222 on observations made over the last 60 years (see Supplementary Material in Fan et al.
 223 (2013)), where around 38% of the WTD are comprised between 1 and 10 *m*).

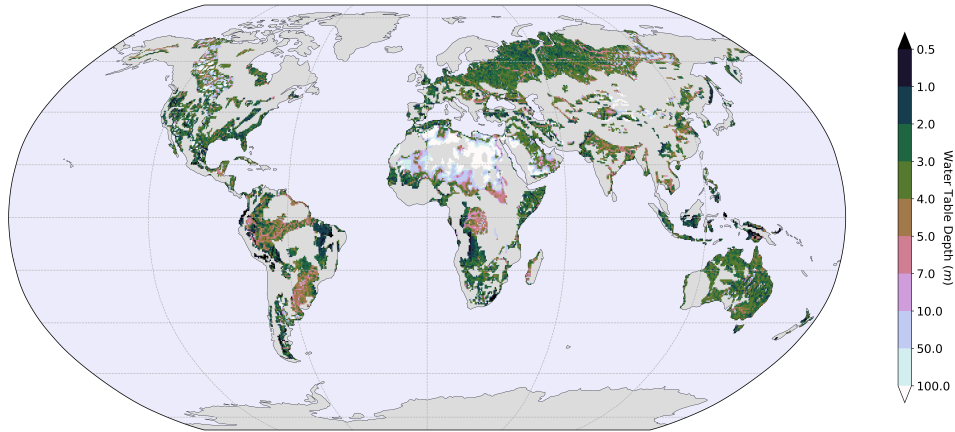


Figure 1. Global distribution of the mean WTD simulated by the CNRM global climate models in the 218 world's major groundwater basins over the present-day period (1985 – 2014) in the historical experiment.

224 In agreement with recent observational studies (IPCC, 2021b), the globally yearly aver-
 225 aged WTD simulated by the CNRM models shows a slight rise over the 1960 to 2014 period
 226 in the historical experiment (Fig.2.A). Following our model estimates, global WTD should
 227 continue to rise with climate change in all future scenarios, at least until 2100 (i.e. the end
 228 of the scenarios). The higher the radiative forcing associated to SSP scenarios, the stronger
 229 the trend of WTD. The AR6 indicates that the global mean annual precipitation over land
 230 is also projected to increase until 2100, in all scenarios (IPCC, 2021c). Precipitation simu-
 231 lated by CNRM models follow the same behavior (Fig.2.B). Overall, the variations of the
 232 simulated global WTD follow those of precipitation, except over the 1950 – 1970 period at
 233 a first glance. During this period, the global mean annual precipitation drops because of
 234 an increase in sulfur emissions in the atmosphere (Wild, 2012). This is not followed by a
 235 decrease of the global mean WTD, even if this decrease is simulated over several regions
 236 such as that of south and southeast Asia (not shown). However, the long-term evolution of
 237 the two variables are highly correlated, with a R-squared of 0.957 between the 5-yr running
 238 means of global WTD and precipitation (not shown).

239 Naturally, this global rising of groundwater due to climate change does not prevent
 240 the occurrence of a depletion in numerous regions. The map on Fig.3.A represents the
 241 relative difference of WTD between present-day climate (1985 – 2014) and the end of the
 242 21st century (2071 – 2100), following the SSP370 scenario. For readability reasons, we chose
 243 to highlight a single scenario (see Supporting Information Fig.S1 for the other scenarios).
 244 We picked the SSP370 because it is one of the scenarios, along with SSP245, which best
 245 match the recent evolution of anthropogenic global fossil-fuel concentrations (Hausfather &
 246 Peters, 2020). Despite a global WTD rising of 3.80%, these results show a clear North-South
 247 dipole in Europe and America between groundwater rising in the north and depletion in
 248 the south (north of the 45° latitude, approximately). The Mediterranean basin, Southern
 249 Africa, Amazonia, central America, Australia and parts of China should experience a strong
 250 groundwater depletion, whilst central Africa, India, Indonesia and eastern Argentina should
 251 see an increase of their groundwater resources with climate change. This spatial pattern
 252 of the WTD changes are the same for all scenarios, the severity of which only impacts the
 253 amplitude of the changes and not their sign.

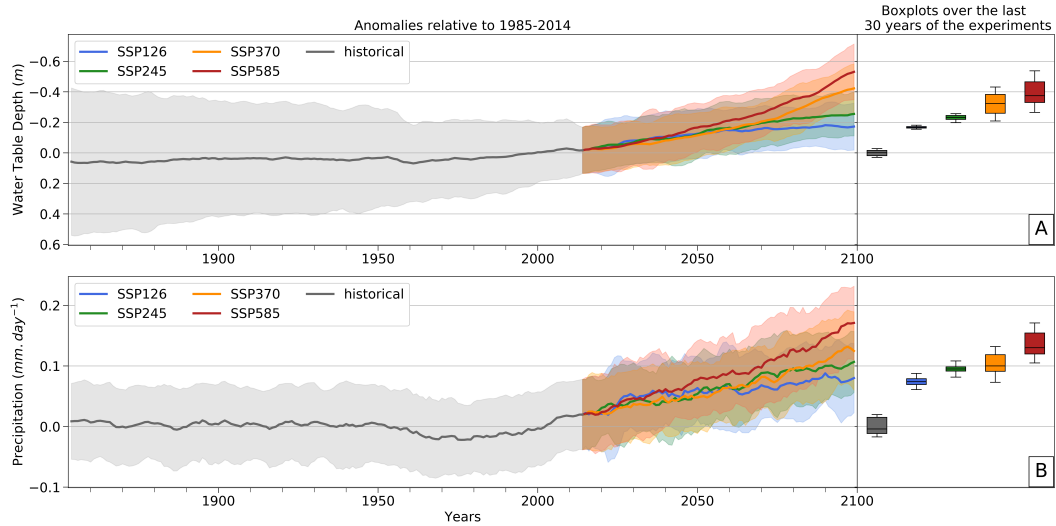


Figure 2. Time series (1850–2100) of the 5-year running average of global mean WTD anomalies (panel **A**) and precipitation over land anomalies (panel **B**), relative to their global average in present-day climate (1985 – 2014 period of the historical experiment), according to all scenarios. The shading areas around the global means represent the inter-member spread (± 1.64 inter-member variance) of each experiment. Boxplots further reflect the inter-member distribution of the last 30 years of the historical experiment (1985 – 2014) and of each scenario (2071 – 2100). On the boxplots, the vertical line indicates the median, the boxplot limits the 1st and 3rd quartiles and the whiskers' length is 1.5 times the interquartile range.

254 Overall, our projections of groundwater levels are consistent with the findings of the
 255 few previous studies based on CMIP5 scenarios which addressed the question of future
 256 groundwater resources at the global scale, using a fully coupled model (Wu et al., 2020) or
 257 global hydrological models run offline (Reinecke et al., 2021).

258 3.2 Climate drivers of the WTD changes

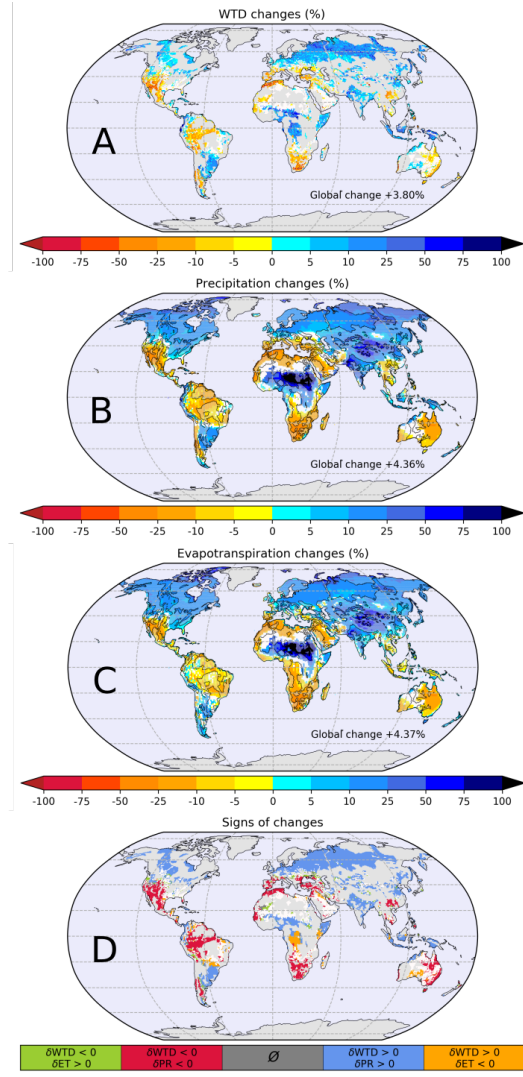


Figure 3. Water Table Depth (A), Precipitation (B) and Evapotranspiration (C) changes (in %) between 1985 – 2014 in the historical experiment and 2071 – 2100 in the SSP370 scenario (the values of the change averaged over land are annotated on the maps). Areas in blue (red) correspond to a future WTD rise (depletion) (A) or an increase (decrease) of precipitation/evapotranspiration (B/C). The white regions correspond to areas where the changes are not statistically significant according to the FDR test (Wilks, 2006, 2016) at a 95% level of confidence. On B and C, the localisation of the groundwater basins is emphasized to facilitate the comparison with WTD (A). D: in red and blue : comparison of the sign of WTD and precipitation (PR) changes ; in yellow and green : comparison of the sign of WTD and evapotranspiration (ET) changes wherever the sign of precipitation changes is not consistent with the sign of WTD changes. The white regions correspond to areas where WTD changes are not statistically significant.

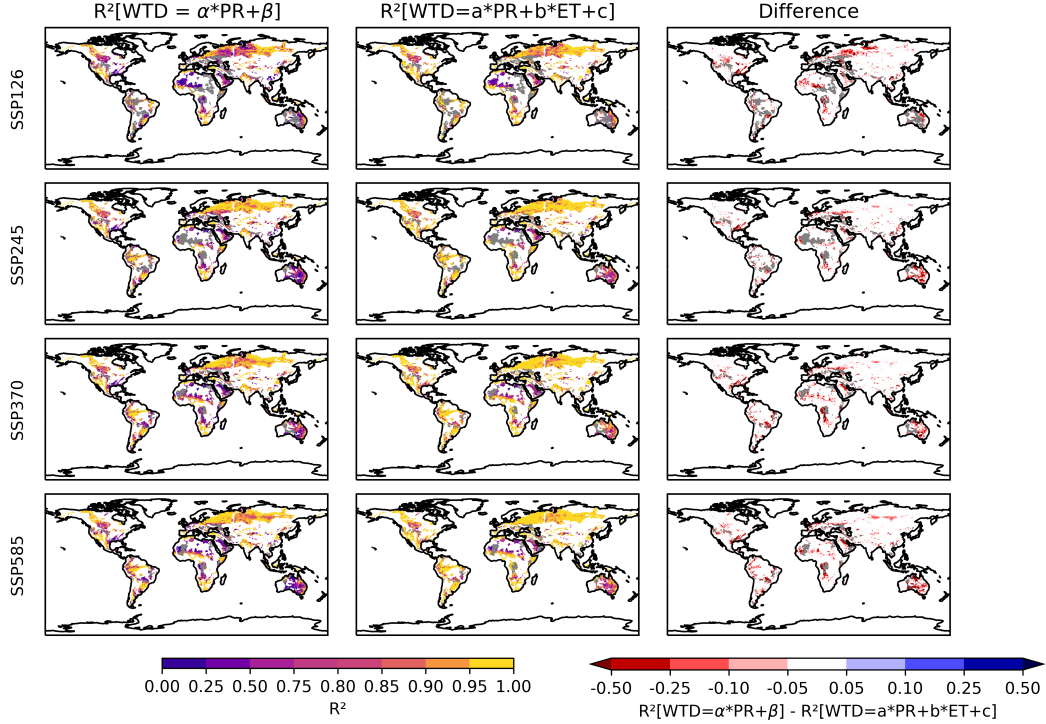


Figure 4. Left panel: R^2 values of the linear regressions for the statistical model $WTD = \alpha * PR + \beta$. The linear regression is computed for each grid point with samples made of the yearly mean values of each variables for each SSP scenarios (i.e. all years from 2014 to 2100). Center panel: Same as left panel but for the statistical model $WTD = a * PR + b * ET + c$. Right panel: R^2 values differences between the second model (center panel) and the first one (left panel). Red areas correspond to areas where WTD changes are better correlated with both precipitation and evapotranspiration changes than with precipitation changes only.

259 Almost everywhere, the sign of WTD changes is determined by the changes of precip-
 260 itation rather than evapotranspiration. Generally, the water table rises if the precipitation
 261 increases and vice versa, whereas an increase (respectively decrease) of evapotranspiration
 262 rarely leads to a depletion (rise) of the aquifer (Fig.3). To further investigate this matter,
 263 two linear regression models were computed for each grid point: the first one links the 5-yr
 264 running mean time-series of WTD with precipitation, and the second one also accounts for
 265 the evapotranspiration time-series. The comparison of the corresponding R-squared (Fig.4)
 266 shows that over most regions, the second regression model is only slightly better than the
 267 first one, given that the correlation between WTD and precipitation is already very high
 268 (R-squared over 0.8) and that evapotranspiration is also highly correlated to precipitation.
 269 In most places therefore, precipitation proves to be the main driver of the WTD long-term
 270 evolution, hence the widespread agreement of signs between the trends of WTD and precip-
 271 itation (blue and red areas on Fig.3.D).

272 There are however a few regions where the inclusion of evapotranspiration in the regres-
 273 sion model considerably improves the rather low R-squared obtained with precipitation
 274 only (Fig.4), which means that evapotranspiration then plays a major role in the evolution
 275 of WTD. This is consistent with previous studies (Condon et al., 2020; Wu et al., 2020)
 276 which stressed the importance of evapotranspiration in the future evolution of groundwa-
 277 ter. The regions where the influence of evapotranspiration prevails correspond to the areas
 278 of disagreement between the precipitation and WTD changes (orange and green areas on

279 Fig.3.D), which are in fact characterized by a lack of significance on the precipitation changes
280 (Fig.3.B). In these cases, either the water table deepens with the increase of evapotranspi-
281 ration (green areas on Fig.3.D) or it rises with the reduction of evapotranspiration (orange
282 areas on Fig.3.D). It is easy to understand how evapotranspiration can increase in a warmer
283 climate. But the decrease of evapotranspiration, in the absence of a significant change of
284 precipitation, is somewhat surprising. Further analysis shows that it is explained by land
285 use change features in SSP scenarios (Hurtt et al., 2020) imposed on the CNRM-ESM2-1
286 model. For example, the deforestation of the Congo Basin in the SSP370 scenario favours
287 groundwater recharge, as it reduces the withdrawal of soil moisture for deep rooted trees
288 transpiration. Indeed, the conversion of forest to agricultural lands can cause an increase in
289 groundwater recharge even if rainfall slightly decreases (Owuor et al., 2016).
290

291 Our analysis of the drivers of WTD changes concerns the aquifers shallower than 100
292 meters in the world's major groundwater basins, which altogether cover 40% of the land
293 surface. However, it is reasonable to assume that aquifers which are not represented in
294 the CNRM models will be driven by the same climate variables (i.e precipitation and evap-
295 otranspiration when precipitation changes are not statically significant). Thus, it seems
296 reasonable to assume that the evolution of the non-represented groundwater basins will
297 mainly follow the precipitation and the evapotranspiration changes.

298

3.3 Multi-model analysis

299

300

301

302

303

304

305

306

307

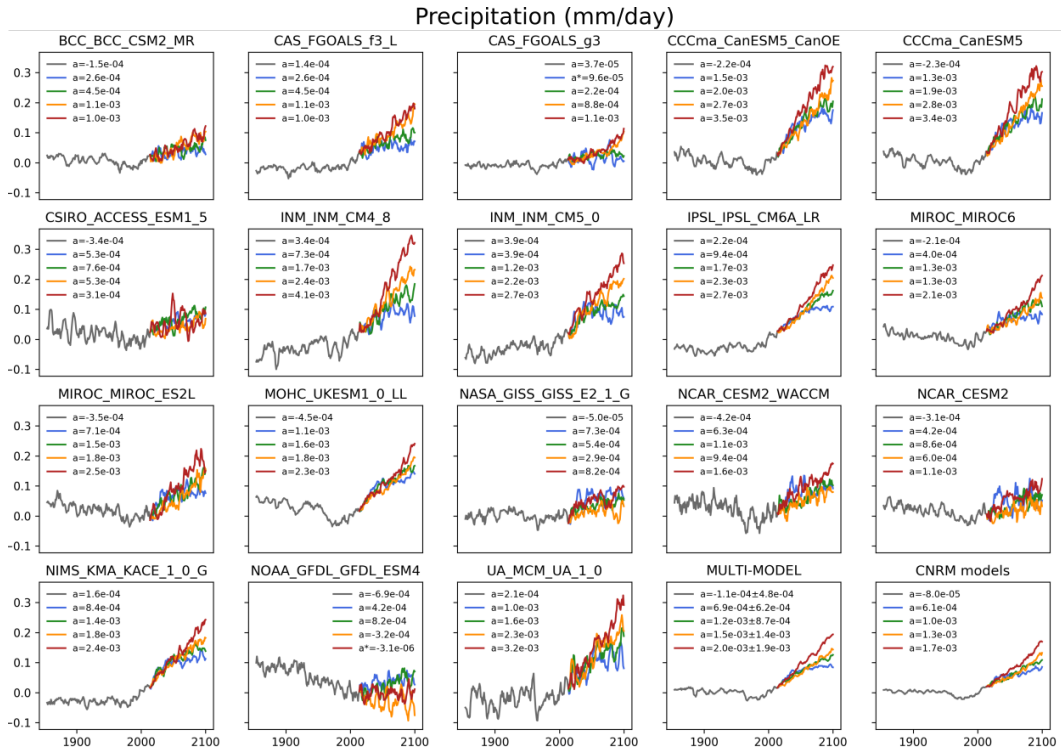


Figure 5. Times-series (1850 – 2100) of the 5-yr running means of global land precipitation anomalies (relatively to 1985 – 2014) for each SSP scenario: ensemble means of the model references in Table1 to the exclusion of the CNRM models, multi-model ensemble of these ensemble means, and ensemble mean of the CNRM models. a is the slope of the linear regression of each time-series. a^* indicates that the slope is not significantly different from 0. The range of the inter-model spread for linear trend of the multi-model ensemble is also given.

308

309

310

311

312

313

314

315

Results of this multi-model analysis show that overall, the CNRM models agree with the other CMIP6 models on the evolution of precipitation and evapotranspiration over land surfaces in the future (Fig.5 and Fig.6). The CNRM models global time-series (1850-2100) fall within the range of the inter-model spread. The spatial patterns of precipitation and evapotranspiration future changes of the CNRM models are also in agreement with the CMIP6 multi-model ensemble results (Fig.7). This naturally reflects the findings already reported in the AR6 (IPCC, 2021a), as well as in the previous IPCC assessment report (IPCC, 2013b). In both cases (CNRM models and CMIP6 ensemble), the future climate

316 is projected to be wetter and more humid in most regions outside of the Mediterranean,
 317 Australia, southern Africa, Brazil and Central America. The few areas where the CNRM
 318 models results disagree with the CMIP6 multi-model mean on the sign of the changes cor-
 319 respond to transition zones between regions of humidification and drying. And in most of
 320 these places, the climate change signal is not statistically significant in the CNRM models.
 321 This agreement between the CNRM models and the CMIP6 multi-model ensembles regard-
 322 ing the climatic drivers of WTD changes provides an increased confidence in our projections
 323 of groundwater levels.

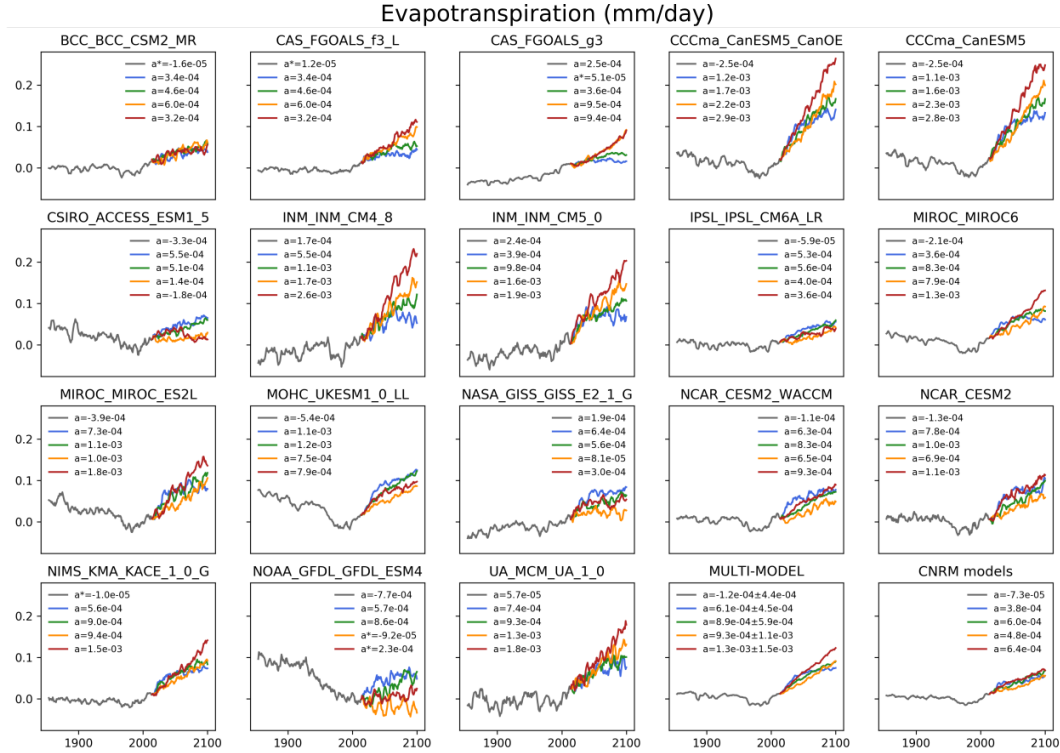


Figure 6. Same as Fig.5 but for evapotranspiration.

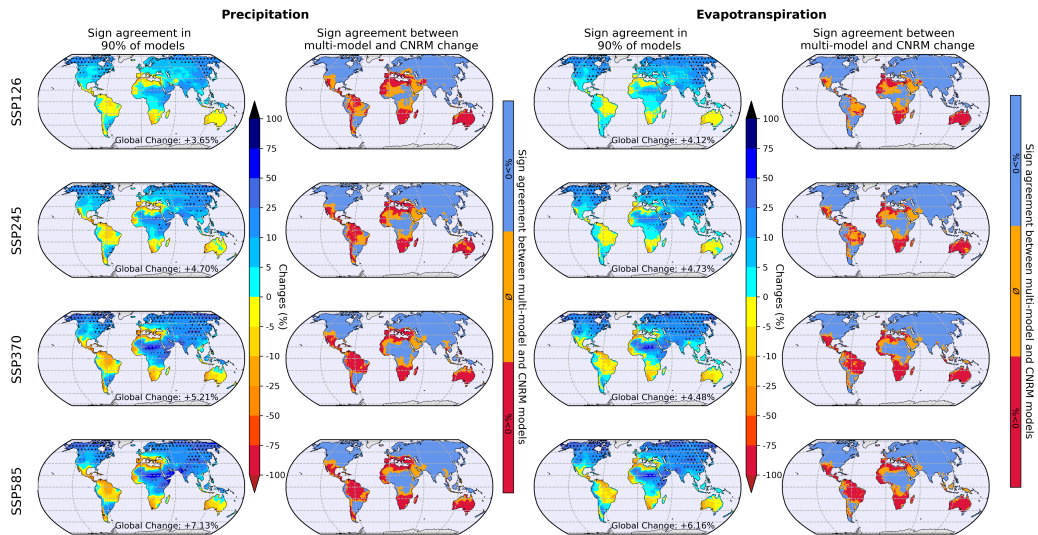


Figure 7. First column: Multi-model ensemble (excluding the CNRM models) of precipitation relative change (in %) between 1985 – 2014 and 2071 – 2100 for each SSP scenario. Black dots indicate areas where 90% of the models agree on the sign of the change. Second column: Comparison of the precipitation multi-model change with the change simulated by the CNRM models. In blue: common increase ; in red: common decrease ; in orange: opposite signs of change. Third and fourth columns: same as the first and second columns but for evapotranspiration.

324

3.4 Potential humans impacts in 2100

325

326

327

328

329

330

331

332

333

334

335

336

337

338

339

Our projections of future groundwater levels can also be analysed in terms of the foreseeable impact on human water risks. To perform the said analysis, we used projections of population densities in 2100 (Supporting Information Fig.S2), which we derived from the current population density (2015) provided by the SocioEconomic Data and Applications Center (SEDAC, 2018) and the projected relative changes of population in each country, provided for each SSP scenario (KC & Lutz, 2017) . The goal is to determine how the population might be impacted by the variation of WTD with climate change. We are aware that because human withdrawals of groundwater are not represented in the CNRM models, our projections of WTD might be somewhat biased, in the sense that some of the simulated future water tables might be shallower than they would be with the inclusion of groundwater pumping. Indeed, it has been shown that pumping can cause or worsen the depletion of aquifer basins (IPCC, 2021a, 2022b; Famiglietti, 2014; Döll et al., 2009; Gurdak, 2017; Scanlon et al., 2012; Wu et al., 2020). The future population densities can also however indicate in which regions the lack of groundwater pumping is more likely to affect our projections of WTD, as the volumes of groundwater withdrawals increase with population density.

340

341

342

343

344

345

346

347

348

Figures 8 and 9 gather the information on WTD and population density in 2100. If we consider the area covered by the world's major groundwater basins we studied here, we find that 39% to 52% (respectively 20% to 26%) of this surface will be affected by a rise (respectively a depletion) of groundwater levels (Fig.8). In terms of population, the global pie chart on Fig.9 indicates that, for the SSP370 scenario, 49% of the population is projected to live across these regions, and is therefore likely to rely on groundwater resources (see Supporting Information Fig.S3 for the other scenario). Among them, 17% (~ 1 billion people) will be affected by groundwater depletion, 68% (~ 4 billion people) will see a rising of groundwater levels, and 15% will experience no significant change. People living outside

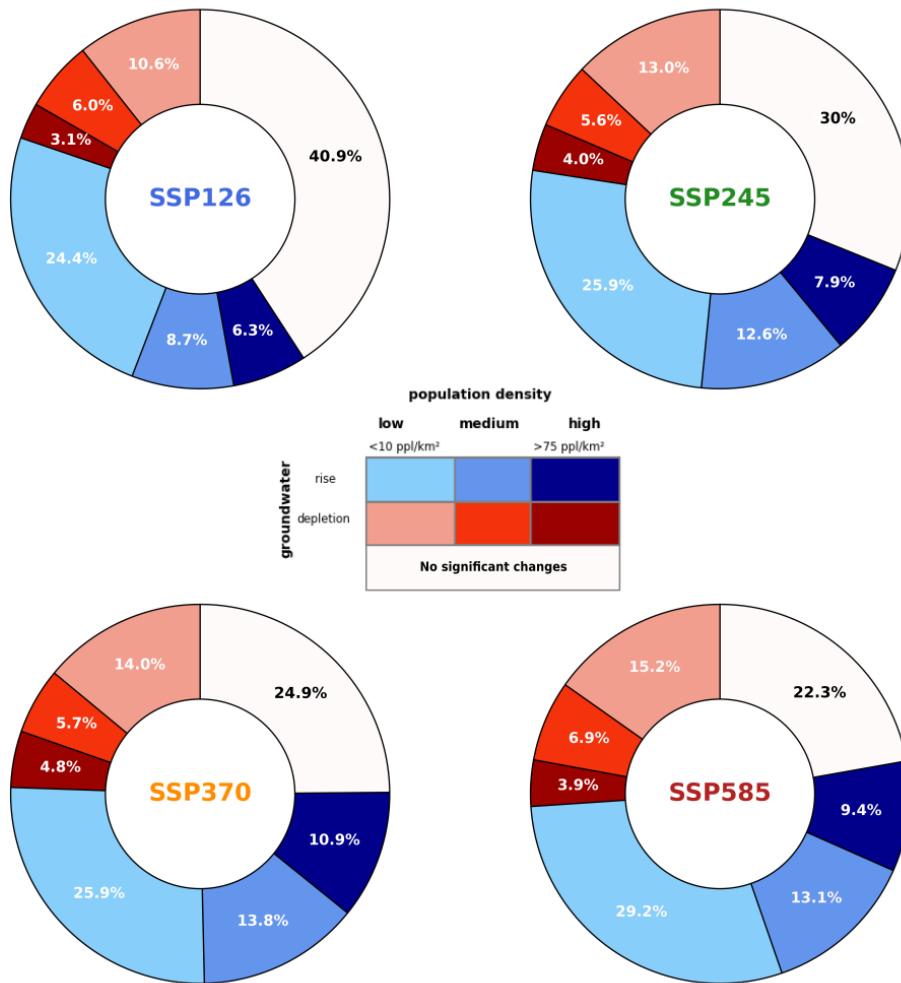


Figure 8. Share of area covered by the world's major groundwater basins where groundwater levels are projected to rise (blue) and to deplete (red). The color intensity indicates the projected population density (people per km²) in 2100. The light colours correspond to areas with fewer than 10 inhabitants per square kilometer and the dark colours to areas with more than 75 inhabitants per square kilometer. The white regions correspond to areas where WTD changes between 1985 – 2014 and 2071 – 2100 are not statistically significant.

349 these large groundwater basins could however still partly rely on groundwater resources,
 350 either because they live near a large aquifer or because they exploit more localised aquifers.
 351 Looking at the results regionally, we find that 16% of the world's population (~2 billion
 352 people) is projected to live in regions where climate change mostly induces a decline of fu-
 353 ture groundwater resources, such as the Mediterranean region or northwest America. And
 354 for the 84% of people living in regions where aquifer levels are mostly projected to rise, the
 355 increase of groundwater resources could be lessened by human withdrawals, or even reverse
 356 into a decrease in the more highly populated areas, such as South Asia.
 357

358 This brings us to the associated water risks, and to the identification of three different
 359 types of situations. The first one corresponds to moderately populated areas where aquifers

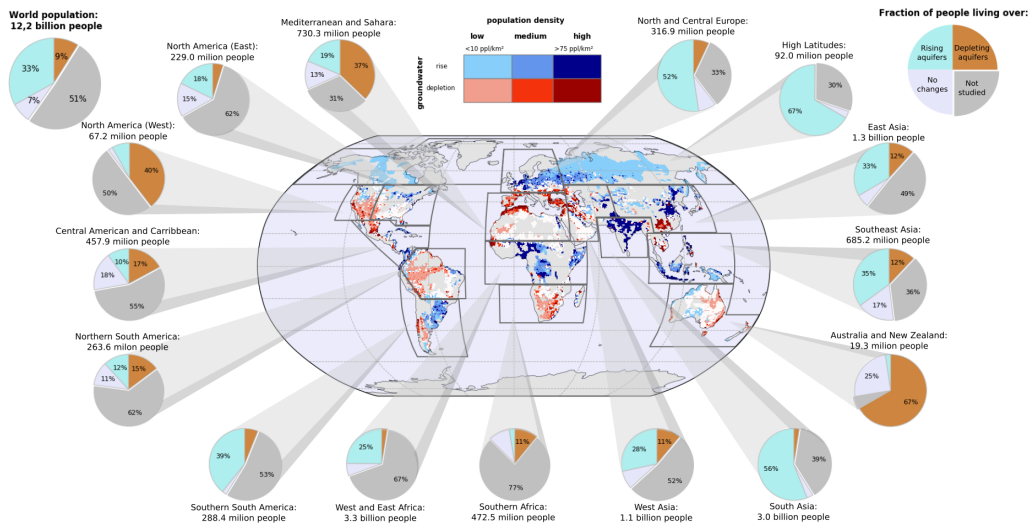


Figure 9. Evolution of WTD and population density in 2100 with the SSP370 scenario. As in Fig.8, aquifer areas are coloured blue (red) if groundwater levels are projected to rise (deepen), whilst the color intensity indicates the projected population density in 2100. The global pie chart (left hand corner) represents the distribution of the world's population which could be affected by a rising (turquoise) or a depletion (brown) of groundwater levels, or which is likely to live above an aquifer basin where future changes are not significant (white) or over unstudied areas (grey). The same pie charts are given for each selected region, defined as those used in the Atlas of Global and Regional Climate Projections in the Annex 1 of the IPCC AR5 (IPCC, 2013a).

360 are projected to rise, such as the high latitudes or parts of Northern Europe. In these regions,
 361 water stress should not be an issue in the future, as the risk of human withdrawal exceeding
 362 the projected increase of groundwater storage can be considered as moderate. There could
 363 however be an increased flood risk, with serious consequences in terms of fatalities, the
 364 destruction of natural areas and human infrastructure. Indeed, the saturation of aquifers
 365 and overlaying soils can foster or worsen spring freshets and floods associated with periods
 366 of intense precipitation.

367 The second case corresponds to highly populated areas such as South Asia or central
 368 Africa, where groundwater levels are also projected to rise. The flood risk might increase in
 369 these regions, as in those previously mentioned. With a high population density however,
 370 human water requirements are expected to be significant and even increase with climate
 371 change and/or the growth of the population. The projected increase of groundwater storage
 372 could therefore be reversed and become a decrease, as is already the case in the North
 373 of India where groundwater is already depleted (Rodell et al., 2009; Panda et al., 2021).
 374 Indeed, India is the country with the highest irrigation from groundwater, and this pumping
 375 constantly increases (Siebert et al., 2010).

376 The third situation corresponds to regions such as the Mediterranean, southern Africa
 377 and southwestern USA. In these moderately to highly populated places, the mean regional
 378 WTD is projected to deepen, corresponding to a depletion of groundwater (even without
 379 taking into account human withdrawal). This could be a huge problem in populated areas
 380 where the drop of WTD will widen the risk of water stress, especially in regions that are
 381 already groundwater-dependant (Iglesias et al., 2007). Again, in these regions, the real fu-
 382 ture depletion should be much stronger than projected, as human withdrawal is not taken

383 into account in the CNRM models.
384

385 4 Summary and prospect

386 The CNRM models provide a spatially contrasted response of groundwater to climate
387 change throughout the 21st century. In all scenarios, the area experiencing a rise in ground-
388 water levels (40 – 50%) is twice the area experiencing a depletion (20 – 25%). Discussing
389 the potential water risks associated with this projected evolution of groundwater levels, we
390 find that depending on the scenario, 0.7 to 1.1 billion people (9% to 11% of the world's
391 population) could be affected by groundwater depletion in 2100 and thus face water scarcity
392 issues. On the contrary, 1.4 to 4 billion people (21% to 33% of the world's population) could
393 see their groundwater resources increase, but this could come at the cost of a higher risk of
394 severe flood events and landslides, due to the seasonal or occasional saturation of aquifers.
395 The confidence in our estimates of the long-term evolution of groundwater level is increased
396 by the agreement between our projections of the main climatic drivers of this evolution
397 (precipitation and evapotranspiration) and the multi-model ensemble of the state-of-the-art
398 CMIP6 models.

399 Nonetheless, to further assess the uncertainties on the groundwater response to future
400 climate change, we argue in favor of a more comprehensive multi-model approach, which
401 would rely on coupled global climate models or Earth system models including a realistic
402 representation of groundwater processes. Other members of the climate and/or hydrology
403 modelling communities have also advocated for the development and use of such holistic
404 global models (Fan et al., 2013; Clark et al., 2015; Boé, 2021; Gleeson et al., 2021). Improv-
405 ing and increasing our confidence in the projections of future groundwater resources does
406 indeed constitute a high-stake issue because it conditions the implementation of suitable mit-
407 igation and adaptation plans to counter the widening risks of water scarcity (Famiglietti,
408 2014; Thomas & Famiglietti, 2019).

409 Beyond the necessity to account for a valuable representation of groundwater pro-
410 cesses in global climate models, we emphasize the need to consider the representation of
411 groundwater pumping and irrigation processes (groundwater contributes to 42% of irrigated
412 water (Döll et al., 2012), which amounts to 70% of human groundwater intake (Siebert et
413 al., 2010)). The consideration of human groundwater withdrawal and its future evolution
414 is likely to modulate, and in some places even invert, the impact of the future climate
415 change on groundwater (Wada, 2016; Wu et al., 2020). This modulation of the groundwater
416 evolution, along with the modification of evapotranspiration and/or hydrological processes
417 induced by irrigation, could affect in return the projected climate, hence the need to include
418 these processes in fully coupled climate models.

419 5 Open Research

420 All the CNRM climate models and multi-model ensemble data are freely available
421 on the ESGF website (<https://esgf-node.ipsl.upmc.fr/search/cmip6-ips1/>). The
422 SEDAC data are available at [https://sedac.ciesin.columbia.edu/data/set/gpw-v4-
423 -population-density-rev11](https://sedac.ciesin.columbia.edu/data/set/gpw-v4-population-density-rev11), the CMIP6 projection of population density by country
424 at <https://tntcat.iiasa.ac.at/SspDb/dsd?Action=htmlpage\&page=30>, the GMTED
425 1km topography data at <https://topotools.cr.usgs.gov/gmted.viewer/>, the global map
426 of the groundwater resources of the world from WHYMAP at <http://www.whymap.org>, and
427 the the principal aquifers of the conterminous United States from the USGS at [https://
428 water.usgs.gov/GIS/metadata/usgswrd/XML/aquifers_us.xml](https://water.usgs.gov/GIS/metadata/usgswrd/XML/aquifers_us.xml).

Acknowledgments

The authors would like to thank Christine Delire, Herve Douville, Julien Boe and Florence Habets for their useful comments. This work is supported by the “Centre National de Recherches Météorologiques” (CNRM) of Météo-France and the “Centre National de la Recherche Scientifique” (CNRS) of the French research ministry. This paper has received support from the European Union’s Horizon 2020 research and innovation programme under Grant Agreement N° 101003536 (ESM2025 – Earth System Models for the Future).

References

- Alley, W. M., Healy, R. W., LaBaugh, J. W., & Reilly, T. E. (2002). Flow and storage in groundwater systems. *Science*, *296*(5575), 1985–1990. doi: 10.1126/science.1067123
- Amanambu, A. C., Obarein, O. A., Mossa, J., Li, L., Ayeni, S. S., Balogun, O., . . . Ochege, F. U. (2020). Groundwater system and climate change: Present status and future considerations. *Journal of Hydrology*, *589*(May), 125163. Retrieved from <https://doi.org/10.1016/j.jhydrol.2020.125163> doi: 10.1016/j.jhydrol.2020.125163
- Boé, J. (2021). The physiological effect of CO₂ on the hydrological cycle in summer over Europe and land-atmosphere interactions. *Climatic Change*, *167*(1-2), 1–20. doi: 10.1007/s10584-021-03173-2
- Cazenave, A., Dieng, H.-b., Meyssignac, B., Schuckmann, K. V., Decharme, B., & Berthier, E. (2014). The rate of sea-level rise. *Nature Climate Change*, *4*(May), 358–361. doi: 10.1038/NCLIMATE2159
- Clark, M. P., Fan, Y., Lawrence, D. M., Adam, J. C., Bolster, D., Gochis, D. J., . . . Maxwell, R. M. (2015). Improving the representation of hydrologic processes in Earth SystemModels. *Water Resources Research*, *51*, 5929–5956. doi: 10.1002/2015WR017096.Received
- Condon, L. E., Atchley, A. L., & Maxwell, R. M. (2020). Evapotranspiration depletes groundwater under warming over the contiguous United States. *Nature Communications*, *11*(1). Retrieved from <http://dx.doi.org/10.1038/s41467-020-14688-0> doi: 10.1038/s41467-020-14688-0
- Decharme, B., Delire, C., Minvielle, M., Colin, J., Vergnes, J. P., Alias, A., . . . Voldoire, A. (2019). Recent Changes in the ISBA-CTrip Land Surface System for Use in the CNRM-CM6 Climate Model and in Global Off-Line Hydrological Applications. *Journal of Advances in Modeling Earth Systems*, *11*(5), 1207–1252. doi: 10.1029/2018MS001545
- Delire, C., Séférian, R., Decharme, B., Alkama, R., Calvet, J. C., Carrer, D., . . . Tzanos, D. (2020). The Global Land Carbon Cycle Simulated With ISBA-CTrip: Improvements Over the Last Decade. *Journal of Advances in Modeling Earth Systems*, *12*(9), 1–31. doi: 10.1029/2019MS001886
- Döll, P., Fiedler, K., & Zhang, J. (2009). Global-scale analysis of river flow alterations due to water withdrawals and reservoirs. *Hydrology and Earth System Sciences*, *13*(12), 2413–2432. doi: 10.5194/hess-13-2413-2009
- Döll, P., Hoffmann-Dobrev, H., Portmann, F. T., Siebert, S., Eicker, A., Rodell, M., . . . Scanlon, B. R. (2012). Impact of water withdrawals from groundwater and surface water on continental water storage variations. *Journal of Geodynamics*, *59-60*, 143–156. Retrieved from <http://dx.doi.org/10.1016/j.jog.2011.05.001> doi: 10.1016/j.jog.2011.05.001
- Douville, H., Ribes, A., Decharme, B., Alkama, R., & Sheffield, J. (2013). Anthropogenic influence on multidecadal changes in reconstructed global evapotranspiration. *Nature Climate Change*, *3*(1), 59–62. Retrieved from <http://dx.doi.org/10.1038/nclimate1632> doi: 10.1038/nclimate1632
- Dürr, H. H., Meybeck, M., & Dürr, S. H. (2005). Lithologic composition of the Earth’s continental surfaces derived from a new digital map emphasizing riverine material transfer. *Global Biogeochemical Cycles*, *19*(4), 1–23. doi: 10.1029/2005GB002515
- Eyring, V., Bony, S., Meehl, G. A., Senior, C. A., Stevens, B., Stouffer, R. J., & Taylor,

- 482 K. E. (2016). Overview of the Coupled Model Intercomparison Project Phase 6
483 (CMIP6) experimental design and organization. *Geoscientific Model Development*,
484 *9*(5), 1937–1958. doi: 10.5194/gmd-9-1937-2016
- 485 Famiglietti, J. S. (2014). The global groundwater crisis. *Nature Climate Change*, *4*(11),
486 945–948. Retrieved from <http://dx.doi.org/10.1038/nclimate2425> doi: 10.1038/
487 nclimate2425
- 488 Fan, Y., Clark, M., Lawrence, D. M., Swenson, S., Band, L. E., & Brantley, S. L.
489 (2019). Hillslope Hydrology in Global Change Research and Earth System Mod-
490 eling Water Resources Research. *Water Resources Research*, *55*, 1737–1772. doi:
491 10.1029/2018WR023903
- 492 Fan, Y., Li, H., & Miguez-Macho, G. (2013). Global patterns of Groundwater Table Depth.
493 *Science*, *339*(6122), 940–943. doi: 10.1126/science.1229881
- 494 Gleeson, T., Wagener, T., Döll, P., Zipper, S. C., West, C., Wada, Y., ... Maxwell, R.
495 (2021). GMD perspective: The quest to improve the evaluation of groundwater rep-
496 resentation in continental- to global-scale models. *Geoscientific Model Development*,
497 *14*(April), 7545–7571.
- 498 Green, T. R., Taniguchi, M., Kooi, H., Gurdak, J. J., Allen, D. M., Hiscock, K. M., ...
499 Aureli, A. (2011). Beneath the surface of global change: Impacts of climate change on
500 groundwater. *Journal of Hydrology*, *405*(3-4), 532–560. doi: 10.1016/j.jhydrol.2011
501 .05.002
- 502 Gurdak, J. J. (2017). Climate-induced pumping. *Nature Geoscience*, *10*.
- 503 Hausfather, Z., & Peters, G. P. (2020). Emissions – the ‘business as usual’ story is misleading.
504 *Nature*, *577*(7792), 618–620. doi: 10.1038/d41586-020-00177-3
- 505 Hurtt, G. C., Chini, L., Sahajpal, R., Frohling, S., Bodirsky, B. L., Calvin, K., ... Hasegawa,
506 T. (2020). Harmonization of global land use change and management for the period
507 850 – 2100 (LUH2) for CMIP6. *Geoscientific Model Development*, *13*, 5425–5464.
- 508 Iglesias, A., Garrote, L., Flores, F., & Moneo, M. (2007). Challenges to manage the
509 risk of water scarcity and climate change in the Mediterranean. *Water Resources*
510 *Management*, *21*(5), 775–788. doi: 10.1007/s11269-006-9111-6
- 511 IPCC. (2013a). Annex I: Atlas of Global and Regional Climate Projections [van Olden-
512 borgh, G.J., M. Collins, J. Arblaster, J.H. Christensen, J. Marotzke, S.B. Power, M.
513 Rummukainen and T. Zhou (eds.)]. In: Climate Change 2013: The Physical Science
514 Basis. Contribution of Working Group I to the Fifth Assessment Report of the In-
515 tergovernmental Panel on Climate Change [Stocker, T.F., D. Qin, G.-K. Plattner, M.
516 Tignor, S.K. Allen, J. Boschung, A. Nauels, Y. Xia, V. Bex and P.M. Midgley (eds.)].
517 Cambridge University Press, Cambridge, United Kingdom and New York, NY, U.
- 518 IPCC. (2013b). Climate Change 2013: The Physical Science Basis. Contribution of Working
519 Group I to the Fifth Assessment Report of the Intergovernmental Panel on Climate
520 Change [Stocker, T.F., D. Qin, G.-K. Plattner, M. Tignor, S.K. Allen, J. Boschung,
521 A. Nauels, Y. Xia, V. Bex and P.M. Midgley (eds.)]. Cambridge University Press,
522 Cambridge, United Kingdom and New York, NY, USA, 1535 pp.
- 523 IPCC. (2021a). Climate Change 2021: The Physical Science Basis. Contribution of Working
524 Group I to the Sixth Assessment Report of the Intergovernmental Panel on Climate
525 Change [Masson-Delmotte, V., P. Zhai, A. Pirani, S.L. Connors, C. Péan, S. Berger,
526 N. Caud, Y. Chen, L. Goldfarb, M.I. Gomis, M. Huang, K. Leitzell, E. Lonnoy, J.B.R.
527 Matthews, T.K. Maycock, T. Waterfield, O. Yelekçi, R. Yu, and B. Zhou (eds.)]. Cam-
528 bridge University Press. In Press.
- 529 IPCC. (2021b). Douville, H., K. Raghavan, J. Renwick, R.P. Allan, P.A. Arias, M. Barlow,
530 R. Cerezo-Mota, A. Cherchi, T.Y. Gan, J. Gergis, D. Jiang, A. Khan, W. Pokam
531 Mba, D. Rosenfeld, J. Tierney, and O. Zolina, 2021: Water Cycle Changes. In Climate
532 Change 2021: The Physical Science Basis. Contribution of Working Group I to the
533 Sixth Assessment Report of the Intergovernmental Panel on Climate Change [Masson-
534 Delmotte, V., P. Zhai, A. Pirani, S.L. Connors, C. Péan, S. Berger, N. Caud, Y. Chen,
535 L. Goldfarb, M.I. Gomis, M. Huang, K. Leitzell, E. Lonnoy, J.B.R. Matthews, T.K.
536 Maycock, T. Waterfield, O. Yelekçi, R. Yu, and B. Zhou (eds.)]. Cambridge University

- 537 Press. In Press.
- 538 IPCC. (2021c). Lee, J.-Y., J. Marotzke, G. Bala, L. Cao, S. Corti, J.P. Dunne, F. En-
 539 gelbrecht, E. Fischer, J.C. Fyfe, C. Jones, A. Maycock, J. Mutemi, O. Ndiaye, S.
 540 Panickal, and T. Zhou:2021, Future Global Climate: Scenario-Based Projections and
 541 Near-Term Information. In *Climate Change 2021: The Physical Science Basis. Contri-
 542 bution of Working Group I to the Sixth Assessment Report of the Intergovernmental
 543 Panel on Climate Change*[Masson-Delmotte, V., P. Zhai, A. Pirani, S.L. Connors, C.
 544 Péan, S. Berger, N. Caud, Y. Chen, L. Goldfarb, M.I. Gomis, M. Huang, K. Leitzell,
 545 E. Lonnoy, J.B.R. Matthews, T.K. Maycock, T. Waterfield, O. Yelekçi, R. Yu, and B.
 546 Zhou (eds.)]. Cambridge University Press. In Press.
- 547 IPCC. (2022a). Caretta, M.A., A. Mukherji, M. Arfanuzzaman, R.A. Betts, A. Gelfan,
 548 Y. Hirabayashi, T.K. Lissner, J. Liu, E. Lopez Gunn, R. Morgan, S. Mwanga, and
 549 S. Supratid, 2022: Water. In: *Climate Change 2022: Impacts, Adaptation, and Vul-
 550 nerability. Contribution of Working Group II to the Sixth Assessment Report of the
 551 Intergovernmental Panel on Climate Change* [H.-O. Pörtner, D.C. Roberts, M. Tignor,
 552 E.S. Poloczanska, K. Mintenbeck, A. Alegría, M. Craig, S. Langsdorf, S. Lösckke, V.
 553 Möller, A. Okem, B. Rama (eds.)]. Cambridge University Press. In Press.
- 554 IPCC. (2022b). IPCC, 2022: *Climate Change 2022: Impacts, Adaptation, and Vulner-
 555 ability. Contribution of Working Group II to the Sixth Assessment Report of the
 556 Intergovernmental Panel on Climate Change* [H.-O. Pörtner, D.C. Roberts, M. Tig-
 557 nor, E.S. Poloczanska, K. Mintenbeck, A. Alegría, M. Craig, S. Langsdorf, S. Lösckke,
 558 V. Möller, A. Okem, B. Rama (eds.)]. Cambridge University Press. In Press.
- 559 Kay, J. E., Deser, C., Phillips, A., Mai, A., Hannay, A., Strand, G., . . . Versteinstein, M.
 560 (2015). The Community Earth System Model (CESM) Large Ensemble Project: a
 561 community resource for studying climate change in the presence of internal climate
 562 variability. *Bulletin of the American Meteorological Society*, 96(August), 1333–1350.
 563 doi: 10.1175/BAMS-D-13-00255.1
- 564 KC, S., & Lutz, W. (2017). The human core of the shared socioeconomic pathways: Pop-
 565 ulation scenarios by age, sex and level of education for all countries to 2100. *Global
 566 Environmental Change*, 42, 181–192. Retrieved from [http://dx.doi.org/10.1016/
 567 j.gloenvcha.2014.06.004](http://dx.doi.org/10.1016/j.gloenvcha.2014.06.004) doi: 10.1016/j.gloenvcha.2014.06.004
- 568 Ledoux, E., Girard, G., & De Marsily, G. (1989). Spatially distributed modelling: con-
 569 ceptual approach, coupling surface water and groundwater, in: *Unsaturated Flow in
 570 Hydrologic Modeling: Theory and Practice. edited by: Morel-Seytoux, H. J.*, 435–454.
- 571 Maxwell, R. M., & Kollet, S. J. (2008). Interdependence of groundwater dynamics and
 572 land-energy feedbacks under climate change. *Nature Geoscience*, 1(10), 665–669. doi:
 573 10.1038/ngeo315
- 574 Meinshausen, M., Vogel, E., Nauels, A., Lorbacher, K., Meinshausen, N., Etheridge, D. M.,
 575 . . . Weiss, R. (2017). Historical greenhouse gas concentrations for climate modelling
 576 (CMIP6). *Geoscientific Model Development*, 10(5), 2057–2116. doi: 10.5194/gmd-10
 577 -2057-2017
- 578 Meixner, T., Manning, A. H., Stonestrom, D. A., Allen, D. M., Ajami, H., Blasch, K. W.,
 579 . . . Walvoord, M. A. (2016). Implications of projected climate change for groundwater
 580 recharge in the western United States. *Journal of Hydrology*, 534, 124–138. Retrieved
 581 from <http://dx.doi.org/10.1016/j.jhydro1.2015.12.027> doi: 10.1016/j.jhydro1.
 582 2015.12.027
- 583 O'Neill, B. C., Kriegler, E., Ebi, K. L., Kemp-Benedict, E., Riahi, K., Rothman, D. S., . . .
 584 Solecki, W. (2017). The roads ahead: Narratives for shared socioeconomic pathways
 585 describing world futures in the 21st century. *Global Environmental Change*, 42, 169–
 586 180. Retrieved from <http://dx.doi.org/10.1016/j.gloenvcha.2015.01.004> doi:
 587 10.1016/j.gloenvcha.2015.01.004
- 588 O'Neill, B. C., Tebaldi, C., Van Vuuren, D. P., Eyring, V., Friedlingstein, P., Hurtt, G., . . .
 589 Sanderson, B. M. (2016). The Scenario Model Intercomparison Project (ScenarioMIP)
 590 for CMIP6. *Geoscientific Model Development*, 9(9), 3461–3482. doi: 10.5194/gmd-9
 591 -3461-2016

- 592 Owuor, S. O., Butterbach-Bahl, K., Guzha, A. C., Rufino, M. C., Pelster, D. E., Díaz-Pinés,
593 E., & Breuer, L. (2016). Groundwater recharge rates and surface runoff response to
594 land use and land cover changes in semi-arid environments. *Ecological Processes*, *5*(1).
595 Retrieved from <http://dx.doi.org/10.1186/s13717-016-0060-6> doi: 10.1186/
596 s13717-016-0060-6
- 597 Padrón, R. S., Gudmundsson, L., Decharme, B., Ducharne, A., Lawrence, D. M., Mao,
598 J., ... Seneviratne, S. I. (2020). Observed changes in dry-season water availability
599 attributed to human-induced climate change. *Nature Geoscience*, *13*(July), 447–481.
600 Retrieved from <http://dx.doi.org/10.1038/s41561-020-0594-1> doi: 10.1038/
601 s41561-020-0594-1
- 602 Panda, D. K., Ambast, S. K., & Shamsudduha, M. (2021). Groundwater depletion in
603 northern India: Impacts of the sub-regional anthropogenic land-use, socio-politics and
604 changing climate. *Hydrological Processes*, *35*(2), 1–16. doi: 10.1002/hyp.14003
- 605 Reinecke, R., Schmied, H. M., Trautmann, T., Andersen, L. S., Burek, P., Flörke, M., ...
606 Pokhrel, Y. (2021). Uncertainty of simulated groundwater recharge at different global
607 warming levels : a global-scale multi-model ensemble study. *Hydrology and Earth
608 System Sciences*, *25*, 787–810.
- 609 Rodell, M., Velicogna, I., & Famiglietti, J. S. (2009). Satellite-based estimates of ground-
610 water depletion in India. *Nature*, *460*(7258), 999–1002. Retrieved from [http://
611 dx.doi.org/10.1038/nature08238](http://dx.doi.org/10.1038/nature08238) doi: 10.1038/nature08238
- 612 Roehrig, R., Beau, I., Saint-Martin, D., Alias, A., Decharme, B., Guérémy, J. F., ... Sénési,
613 S. (2020). The CNRM Global Atmosphere Model ARPEGE-Climat 6.3: Description
614 and Evaluation. *Journal of Advances in Modeling Earth Systems*, *12*(7), 1–53. doi:
615 10.1029/2020MS002075
- 616 Scanlon, B. R., Faunt, C. C., Longuevergne, L., Reedy, R. C., Alley, W. M., McGuire, V. L.,
617 & McMahon, P. B. (2012). Groundwater depletion and sustainability of irrigation
618 in the US High Plains and Central Valley. *Proceedings of the National Academy of
619 Sciences of the United States of America*, *109*(24), 9320–9325. doi: 10.1073/pnas
620 .1200311109
- 621 Scanlon, B. R., Keese, K. E., Flint, A. L., Flint, L. E., Gaye, C. B., Edmunds, W. M., &
622 Simmers, I. (2006). Global synthesis of groundwater recharge in semiarid and arid
623 regions. *Hydrological Processes*, *20*(15), 3335–3370. doi: 10.1002/hyp.6335
- 624 SEDAC. (2018). Center for International Earth Science Information Network - CIESIN
625 - Columbia University. 2018. Gridded Population of the World, Version 4 (GPWv4):
626 Population Density, Revision 11. Palisades, NY: NASA Socioeconomic Data and Appli-
627 cations Center (SEDAC). <https://doi.org/10.7927/H49C6VHW>. Accessed 18/03/21.
- 628 Séférian, R., Nabat, P., Michou, M., Saint-Martin, D., Voltaire, A., Colin, J., ... Madec,
629 G. (2019). Evaluation of CNRM Earth System Model, CNRM-ESM2-1: Role of
630 Earth System Processes in Present-Day and Future Climate. *Journal of Advances in
631 Modeling Earth Systems*, *11*(12), 4182–4227. doi: 10.1029/2019MS001791
- 632 Siebert, S., Burke, J., Faures, J. M., Frenken, K., Hoogeveen, J., Döll, P., & Portmann,
633 F. T. (2010). Groundwater use for irrigation - A global inventory. *Hydrology and
634 Earth System Sciences*, *14*(10), 1863–1880. doi: 10.5194/hess-14-1863-2010
- 635 Taylor, K. E., Stouffer, R. J., & Meehl, G. A. (2012). An Overview of CMIP5 and the
636 experiment design. *Amer. Meteor. Soc.*, *93*, 1333–1349. doi: 10.1175/BAMS-D-11
637 -00094.1
- 638 Taylor, R. G., Scanlon, B., Döll, P., Rodell, M., Van Beek, R., Wada, Y., ... Treidel, H.
639 (2013). Ground water and climate change. *Nature Climate Change*, *3*(4), 322–329.
640 doi: 10.1038/nclimate1744
- 641 Thomas, B. F., & Famiglietti, J. S. (2019). Identifying Climate-Induced Groundwater
642 Depletion in GRACE Observations. *Scientific Reports*, *9*(1), 1–9. Retrieved from
643 <http://dx.doi.org/10.1038/s41598-019-40155-y>
- 644 Vergnes, J.-P. (May 2014). Développement d'une modélisation hydrologique incluant la
645 représentation des aquifères : évaluation sur la France et à l'échelle globale. *PhD
646 thesis (Institut National Polytechnique de Toulouse)*.

- 647 Vergnes, J. P., & Decharme, B. (2012). A simple groundwater scheme in the TRIP river
648 routing model: Global off-line evaluation against GRACE terrestrial water storage
649 estimates and observed river discharges. *Hydrology and Earth System Sciences*, *16*(10),
650 3889–3908. doi: 10.5194/hess-16-3889-2012
- 651 Vergnes, J. P., Decharme, B., Alkama, R., Martin, E., Habets, F., & Douville, H. (2012).
652 A simple groundwater scheme for hydrological and climate applications: Description
653 and offline evaluation over France. *Journal of Hydrometeorology*, *13*(4), 1149–1171.
654 doi: 10.1175/JHM-D-11-0149.1
- 655 Vergnes J.P., Decharme B, H. F. (2014). Introduction of groundwater capillary rises using
656 subgrid spatial variability of topography into the ISBA land surface model. *Journal*
657 *of Geophysical Research*(119), 11,065–11,086. doi: 10.1002/2014JD021573.Received
- 658 Voldoire, A., Saint-Martin, D., S en esi, S., Decharme, B., Alias, A., Chevallier, M., ...
659 Waldman, R. (2019). Evaluation of CMIP6 DECK Experiments With CNRM-CM6-
660 1. *Journal of Advances in Modeling Earth Systems*, *11*(7), 2177–2213. doi: 10.1029/
661 2019MS001683
- 662 Wada, Y. (2016). Impacts of Groundwater Pumping on Regional and Global Water
663 Resources. *Terrestrial Water Cycle and Climate Change*(May 2016), 337. doi:
664 10.1007/978-3-319-32449-4
- 665 Wada, Y., Van Beek, L. P., Sperna Weiland, F. C., Chao, B. F., Wu, Y. H., & Bierkens,
666 M. F. (2012). Past and future contribution of global groundwater depletion to sea-level
667 rise. *Geophysical Research Letters*, *39*(9), 1–6. doi: 10.1029/2012GL051230
- 668 Wild, M. (2012). Enlightening global dimming and brightening. *Bulletin of the American*
669 *Meteorological Society*, *93*(1), 27–37. doi: 10.1175/BAMS-D-11-00074.1
- 670 Wilks, D. S. (2006). On "field significance" and the False Discovery Rate. *Journal of Applied*
671 *Meteorology and Climatology*, *45*(9), 1181–1189. doi: 10.1175/JAM2404.1
- 672 Wilks, D. S. (2016). "The stippling shows statistically significant grid points": How research
673 results are routinely overstated and overinterpreted, and what to do about it. *Bulletin*
674 *of the American Meteorological Society*, *97*(12), 2263–2273. doi: 10.1175/BAMS-D-15-
675 -00267.1
- 676 Wu, W.-Y., Lo, M.-h., Wada, Y., Famiglietti, J. S., Reager, J. T., Yeh, P. J., ... Yang,
677 Z.-L. (2020). Divergent effects of climate change on future groundwater availability in
678 key mid-latitude aquifers. *Nature Communications*, *11*, 1–9. Retrieved from [http://](http://dx.doi.org/10.1038/s41467-020-17581-y)
679 dx.doi.org/10.1038/s41467-020-17581-y doi: 10.1038/s41467-020-17581-y